Application of "parallel" moiré deflectometry and the single beam Z-scan technique in the measurement of the nonlinear refractive index

Saifollah Rasouli,[1,2,*] H. Ghasemi,[1] M. T. Tavassoly,[2,3] and H. R. Khalesifard[1,2]

[1]Department of Physics, Institute for Advanced Studies in Basic Sciences (IASBS), Zanjan 45137-66731, Iran

[2]Optics Research Center, Institute for Advanced Studies in Basic Sciences (IASBS), Zanjan 45137-66731, Iran

[3]Physics Department, University of Tehran, Kargar Shomally Avenue, Tehran 14399-66951, Iran

*Corresponding author: rasouli@iasbs.ac.ir

Received 18 November 2010; accepted 28 March 2011;
posted 5 April 2011 (Doc. ID 138369); published 23 May 2011

In this paper, the application of "parallel" moiré deflectometry in measuring the nonlinear refractive index of materials is reported. In "parallel" moiré deflectometry the grating vectors are parallel, and the resulting moiré fringes are also parallel to the grating lines. Compared to "rotational" moiré deflectometry and the Z-scan technique, which cannot easily determine the moiré fringe's angle of rotation and is sensitive to power fluctuations, respectively, "parallel" moiré deflectometry is more reliable, which allows one to measure the radius of curvature of the light beam by measuring the moiré fringe spacing. The nonlinear refractive index of the sample, including the sense of the change, is obtained from the moiré fringe spacing curve. The method is applied for measuring the nonlinear refractive index of ferrofluids.

OCIS codes: 190.0190, 120.4120, 110.6760, 190.4400.

1. Introduction

One of the convenient methods for the measurement of the nonlinear refractive index, n_2, is the Z-scan technique [1,2]. In this technique a single focused Gaussian laser beam is prepared. The sample is moved along the propagation direction, z, in the focal region of the beam. The beam power propagating through a small aperture at the far field is measured as a function of sample position. This provides necessary data for determination of the nonlinearity.

In the presence of a nonlinear sample near the focal plane of a Gaussian laser beam in a tight-focus limiting geometry, the optical-field-induced refractive index changes in medium and leads to the well-known self-focusing or defocusing (self-lensing) effect. As a result, the radius of curvature of the laser beam is changed due to the self-lensing effect. In this paper we have used "parallel" moiré deflectometry to measure the radius of curvature of the laser beam as a function of the sample position. In "parallel" moiré deflectometry the grating vectors are parallel, and the resulting moiré fringes are also parallel to the gratings lines. It should be mentioned that spatial analysis of the thermal lens [3] and measurement of the nonlinear refractive index [4] have been reported using moiré deflectometry. In the first work analysis was based on the measurement of the minimum intensity of the moiré fringes, and the second work was based on the measurement of the moiré fringe's rotation angle. The main advantage of our method is the measurement of the radius of curvature of the beam by measuring the moiré fringe period. This method is more reliable compared to "rotational" moiré deflectometry, which cannot easily determine the moiré fringe's angle of rotation [4–13]. Also, compared to the classic Z-scan technique, it has the advantage of being insensitive to the beam

0003-6935/11/162356-05$15.00/0

pointing instability and is insensitive to the power fluctuations.

2. Experimental Setup

A schematic diagram of the experimental setup is shown in Fig. 1. A laser beam is focused by a lens and is recollimated by another lens, then strikes a grating. In the presence of a sample near the focal point of the first lens, the radius of curvature of the beam is changed due to the self-lensing effect. By superposing a similar grating on one of the self-images of the first grating, for the case where the gratings vectors are parallel to each other, the "parallel" moiré fringes are formed just due to the beam divergence or convergence. The sample is moved along the light beam, and the moiré fringes corresponding to the different positions of the sample are recorded. The nonlinear refractive index of the sample and its sign are obtained from the moiré fringe spacing curve.

3. Theoretical Framework

In the theoretical considerations we assume that at the focal plane of the first lens $L1, z = 0$, we know the beam waist w_0 of Gaussian beam and the thin nonlinear sample is modeled as a thin lens of focal length $f_s(z)$ that is located at z. The refractive index of the sample, n, which depends on the radiation intensity, may be expressed in terms of the nonlinear refractive index, n_2, through $n(\rho,z) = n_0 + n_2 I(\rho,z) = n_0 + \Delta n(\rho,z)$, where n_0 is the linear index of refraction, $I(\rho,z)$ is the irradiance of the laser beam within the sample, $\Delta n(\rho,z)$ is the light-induced refractive index change, and ρ is the radial coordinate. For the Gaussian beam traveling in the $+z$ direction, we can write the beam irradiance as

$$I(\rho,z) = I_0 \frac{w_0^2}{w^2(z)} \exp\left[-\frac{2\rho^2}{w^2(z)}\right], \tag{1}$$

where w_0 and I_0 are the beam waist and the beam irradiance at the focus, respectively, $w(z) = w_0(1 + z^2/z_0^2)^{1/2}$ is the beam radius at z, $z_0 = \pi w_0^2/\lambda$ is the diffraction length of the beam, and λ is the laser wavelength. For the Gaussian laser beam, the radial dependence of the irradiance gives rise to a radially dependent refractive index change near the beam axis by

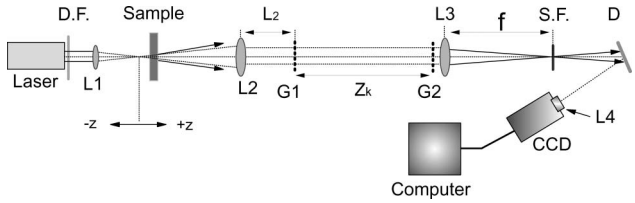

Fig. 1. Schematic diagram of the experimental setup. *D.F.*, *L*1, *L*2, *G*1, *G*2, *L*3, *S.F.*, *D*, and *L*4 stand for neutral density filter, focusing lens, collimating lens, first grating, second grating, Fourier transforming lens, spatial filter, diffuser, and imaging lens, respectively.

$$\Delta n(\rho,z) = n_2 I_0 \frac{w_0^2}{w^2(z)} \exp\left[-\frac{2\rho^2}{w^2(z)}\right]. \tag{2}$$

In the parabolic approximation one can rewrite Eq. (2) in following form:

$$\Delta n(\rho,z) \approx n_2 I_0 \frac{w_0^2}{w^2(z)} \left[1 - \frac{2\rho^2}{w^2(z)}\right]. \tag{3}$$

For a thin nonlinear medium of thickness s, near the beam axis the parabolic approximation yields a thin spherical lens with an effective focal length of

$$f_s(z) = \frac{\pi w^4(z)}{8 n_2 s P} = f_s(0)\left(1 + \frac{z^2}{z_0^2}\right)^2, \tag{4}$$

where $f_s(0)$ is defined as the induced effective focal length at the focus. In the derivation of Eq. (4) we have used the transmission phase function of a positive thin lens $-\frac{2\pi}{\lambda}\frac{\rho^2}{2f}$ [14] and $I_0 = 2P/\pi w_0^2$, where P is the laser power and f is the focal length of lens. Compared to Eq. (4) of [4], there is a mistake in the derivation of Eq. (4) of [4], where the factor 4 should be replaced by 8 in the denominator [15].

The laser beam, after propagation through the sample, is recollimated by the second lens, $L2$, when the sample is placed just at the focal plane of $L1$. Then the beam illuminates two gratings $G1$ and $G2$ of equal periods d, separated by Z_k along the optical axis. The grating vectors are parallel to each other and are perpendicular to the optical axis of the setup. The parameter Z_k denotes the kth Talbot's distance for the $G1$. Moving the sample from $z = 0$ causes the location of the focal point to move and correspondingly changes the radius of curvature of the beam on $G1$. In this case, the spatial period of the self-image is magnified by $\frac{r+Z_k}{r}$, where r is the radius of curvature of the laser beam at the $G1$ plane [16]. More detail and a new application of this kind of moiré fringes are presented in [16]. It should be mentioned that r is positive when the beam on the $G1$ plane is divergent and is negative when the beam is convergent. In the $G2$ plane, a multiplicative moiré pattern will appear by superposition of the kth self-image of $G1$, with period $d \pm \delta d$, and $G2$, with period d. Here the "+" and the "–" signs correspond to the divergent and convergent beams, respectively. In this case the spatial period of the moiré fringes is obtained by

$$d_m = \frac{d^2}{\delta d}, \tag{5}$$

and the moiré fringes are parallel to the grating rulings. Using $\delta d = \frac{Z_k}{|r|} d$ in Eq. (5), we get

$$d_m = \frac{|r| d}{Z_k}. \tag{6}$$

Thus, d_m depends on the radius of curvature of the beam. When the beam is focused on $G1$, d_m is equal

to zero. This case, for a sample having $n_2 < 0$, is obtained on the $-z$ side of the focus. Now let us describe the propagation of the beam through $L1$ (with focal length f_1), the sample (with an effective focal length $f_s(z)$), $L2$ (with focal length f_2), and the distances between them using the ray tracing procedure. By using the transfer matrices of lenses and free spaces, the *ABCD* matrices of the system would be

$$\begin{pmatrix} A & B \\ C & D \end{pmatrix} = \begin{pmatrix} 1 & 0 \\ \frac{-1}{f_2} & 1 \end{pmatrix} \begin{pmatrix} 1 & f_2 - z \\ 0 & 1 \end{pmatrix} \begin{pmatrix} 1 & 0 \\ \frac{-1}{f_s(z)} & 1 \end{pmatrix} \times \begin{pmatrix} 1 & f_1 + z \\ 0 & 1 \end{pmatrix} \begin{pmatrix} 1 & 0 \\ \frac{-1}{f_1} & 1 \end{pmatrix}. \quad (7)$$

The effective focal length, *EFL*, of a system is the distance from the principal point to the focal point. The back focal length, *BFL*, or back focus is the distance from the vertex of the last surface of the system to the second focal point. From the theory of the *ABCD* matrices, the focal length of a system and the EFL – BFL are given by $f_t = \frac{-1}{C}$ and $S = \frac{1-A}{C}$, respectively [17]. According to the configuration of Fig. 1, the radius of curvature of the beam on $G1$ can be written as

$$r(z) = L_2 - S(z) - f_t(z), \quad (8)$$

where L_2 is the distance of the $L2$ and $G1$, and $S(z)$ is the distance of the exit plane and the second principal plane of the complex optical system. After some calculations, we obtain

$$r(z) = L_2 + \frac{f_2^2}{z} - \frac{f_s(z) f_2^2}{z^2} - f_2. \quad (9)$$

Finally, using Eqs. (4) and (9) in Eq. (6), we have

$$d_m(z) = \frac{d}{Z_k} \left| \left\{ L_2 + \frac{f_2^2}{z} - \frac{f_2^2}{z^2} f_s(0) \left(1 + \frac{z^2}{z_0^2} \right)^2 - f_2 \right\} \right|. \quad (10)$$

Equation (10) shows that when the sample is placed at the focus ($z = 0$), the moiré fringe spacing will be infinite. Furthermore, it shows there is a local nonzero minimum value for d_m in the $+z$ side of the focus (for $f_s < 0$) or in the $-z$ side (for $f_s > 0$). By measuring the moiré fringe spacing at various sample positions, using Eq. (10) $f_s(0)$ will be obtained. Finally, using Eq. (4), n_2 will be determined.

4. Experimental Results

We have examined the technique for measuring the nonlinear refractive index in ferrofluids, Au nanoparticles, and neutral red organic dye. In this work, we refer to the measurements we performed on a 2 mM concentration of ferrofluids (EFH1 from Ferro Tec.) in thinner solution in a 1 mm thick cell. The second harmonic of a 70 mW cw diode pumped Nd:YAG laser beam passes through a double lens telescopic system

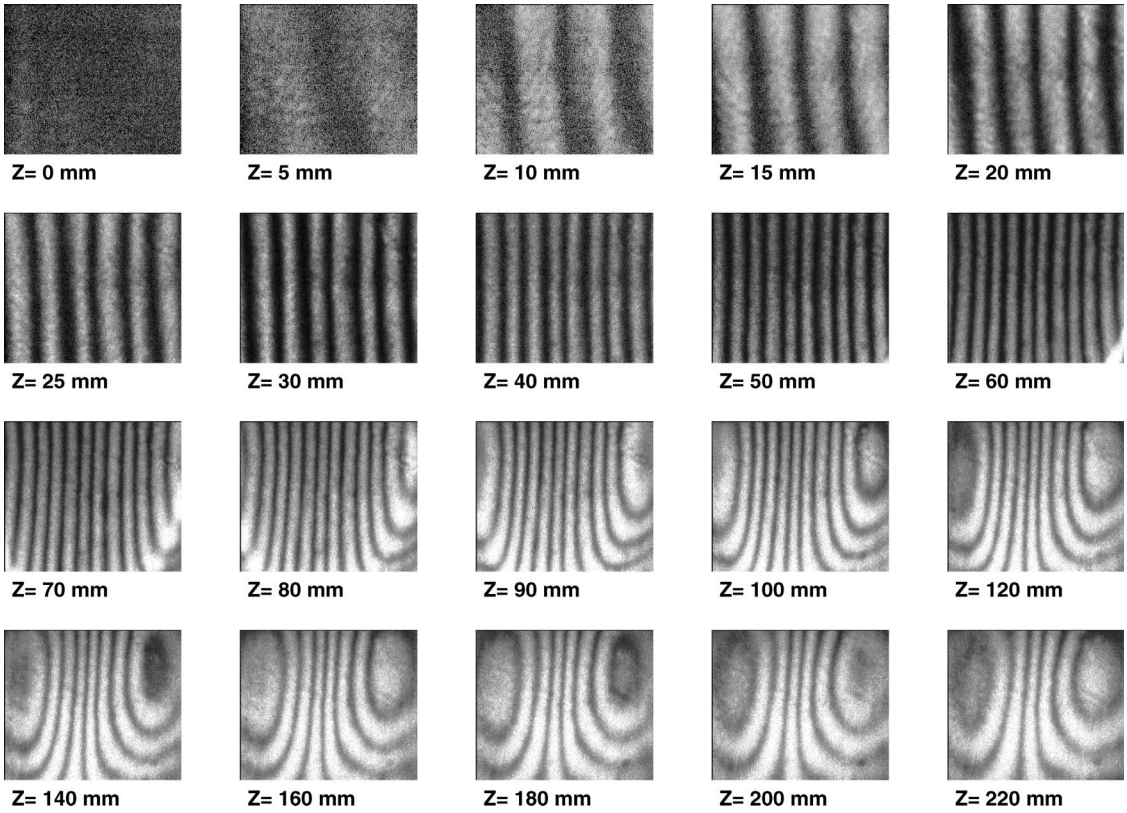

Fig. 2. Typical moiré patterns recorded at different distances of the sample from the focal plane for laser power 70 mW. The corresponding video can be observed in the background (Media 1 DVI, 1.79 MB).

and strikes $G1$. The distance between planes of $G1$ and $G2$ is chosen as 77 mm. The gratings $G1$ and $G2$ with the period of 1/100 mm were installed on suitable mounts. The holders of the gratings could be rotated around the optical axis to adjust the angle between the gratings. The lens $L3$ forms the Fourier transform of the moiré pattern on its second focal plane. Using a suitable spatial filter in the focal plane of $L3$, the unwanted frequencies are removed. A diffuser D is installed after the spatial filter. The image of the moiré pattern is projected on a CCD camera by lens $L4$. The projecting lens, $L4$, is equipped with a variable aperture diaphragm to avoid CCD saturation. For some applications, one can replace the diffuser D in Fig. 1 with the CCD and record the moiré pattern directly.

The sample is moved along the z direction of the beam, and the moiré fringes corresponding to the different positions of the sample are recorded and stored in a computer. Figure 2 shows typical frames of the moiré fringes patterns that were recorded in the $+z$ side of the focus for the laser power 70 mW. The background movie (Media 1) of Fig. 2 contains all of the moiré patterns that were recorded in $+z$ side of the focus. We have observed the $d_m = 0$ case on the $-z$ side of the focus and a nonzero minimum value for d_m on the $+z$ side of the focus. Thus, according to Eqs. (10) and (4), the signs of f_s and n_2 of the sample obtained are negative. This result is also obtained directly by fitting Eq. (10) on the experimental values of d_m.

In Fig. 3 measured Z-scan values of the moiré fringe period are plotted for two laser powers, 25 and 70 mW. For the experimental values $Z_k = 77$ mm, $f_1 = 75$ mm, $f_2 = 585$ mm, $L_2 = 265$ mm, $d = 1/100$ mm, and $w_0 = 31\,\mu$m, the mean value of n_2 obtained from a series of independent experiments is $-(2.2 \pm .1) \times 10^{-4}\,\mathrm{cm^2\,W^{-1}}$. This error takes into account not only the fitting errors but also the reproducibility of the experiment. The order of magnitude of n_2 is compatible with the typical value obtained by other techniques [18].

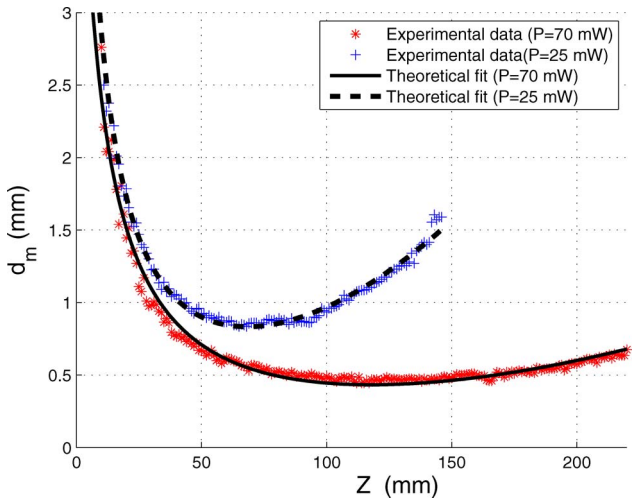

Fig. 3. (Color online) Behavior of moiré fringe period at various z, with theoretical fits on the experimental data for two laser powers, 25 and 70 mW.

5. Conclusion

"Parallel" moiré deflectometry is used to measure the nonlinear refractive index in materials. We have measured the curvature of the laser beam and, as a result, the nonlinear refractive index of the sample by measuring the moiré fringe spacing in a Z-scan setup equipped with a moiré deflectometer. Compared to "rotational" moiré deflectometry, measurement of the moiré fringe spacing is more accurate than the rotation measurement. This method is also more reliable than the Z-scan technique that is based on power measurements, because in this method we do not need to use precise power detectors. In addition, there are major disadvantages associated with the Z-scan technique. For example, the Z-scan curve is distorted by misalignment, sample imperfections, and laser beam power fluctuation during the measurement. Finally, by suitable selection of grating period and the distance between the gratings, one can adjust the precision of the method according to the nonlinearity of the sample.

The authors thank Yasser Rajabi for some useful help in setup arrangement. Also, the authors acknowledge A. Javadi and F. Kabiri for some useful help in sample preparation.

References

1. M. Sheik-bahae, A. A. Said, and E. W. Van Stryland, "High-sensitivity, single-beam n2 measurements," Opt. Lett. **14**, 955–957 (1989).
2. M. Sheik-bahae, A. A. Said, T. Wei, D. J. Hagan, and E. W. Van Stryland, "Sensitive measurement of optical nonlinearities using a single beam," IEEE J. Quantum Electron. **26**, 760–769 (1990).
3. I. Glatt, Z. Karny, and O. Kafri, "Spatial analysis of the CO2 laser-induced thermal lens in SF_6 by moiré deflectometry," Appl. Opt. **23**, 274–277 (1984).
4. K. Jamshidi-Ghaleh and N. Mansour, "Nonlinear refraction measurements of materials using the moiré deflectometry," Opt. Commun. **234**, 419–425 (2004).
5. M. H. Majles Ara, S. H. Mousavi, E. Koushki, S. Salmani, A. Gharibi, and A. Ghanadzadeh, "Nonlinear optical responses of Sudan IV doped liquid crystal by z-scan and moiré deflectometry techniques," J. Mol. Liq. **142**, 29–31 (2008).
6. M. H. Majles Ara, E. Koushki, S. H. Mousavi, S. Salmani, M. Rafizadeh, and A. Gharibi, "Nonlinear optical properties of a dithiooxamide determined by single beam techniques," Mater. Chem. Phys. **109**, 320–324 (2008).
7. M. H. Majles Ara, S. H. Mousavi, S. Salmani, and E. Koushki, "Measurement of nonlinear refraction of dyes doped liquid crystal using moiré deflectometry," J. Mol. Liq. **140**, 21–24 (2008).
8. S. S. Lin, "Optical properties of TiO2 nanoceramic films as a function of NAl co-doping," Ceram. Int. **35**, 2693–2698 (2009).
9. S. S. Lin, Y. H. Hung, and S. C. Chen, "Optical properties of TiO2 thin films deposited on polycarbonate by ion beam assisted evaporation," Thin Solid Films **517**, 4621–4625 (2009).
10. S. S. Lin and D. K. Wu, "The properties of Al-doped TiO2 nanoceramic films deposited by simultaneous rf and dc magnetron sputtering," Ceram. Int. **36**, 87–91 (2010).

11. S. S. Lin, S. C. Chen, and Y. H. Hung, "TiO2 nanoceramic films prepared by ion beam assisted evaporation for optical application," Ceram. Int. **35**, 1581–1586 (2009).
12. S. S. Lin, Y. H. Hung, and S. C. Chen, "The properties of TiO2 nanoceramic films prepared by electron beam evaporation," J. Nanosci. Nanotechnol. **9**, 3599–3605 (2009).
13. S. S. Lin and D. K. Wu, "Enhanced optical properties of TiO2 nanoceramic films by oxygen atmosphere," J. Nanosci. Nanotechnol. **10**, 1099–1104 (2010).
14. S. A. Akhmanov and S. Yu. Nikitin, *Physical Optics* (Clarendon, 1997), pp. 320–322.
15. S. Rasouli and K. Jamshidi-Ghaleh, "Erratum to 'Nonlinear refraction measurements of materials using the moiré deflectometry' [K. Jamshidi-Ghaleh, N. Mansour, Opt. Commun. 234, 419 (2004)]," Opt. Commun. **284**, 1481–1482 (2011).
16. S. Rasouli and M. T. Tavassoly, "Application of the moiré deflectometry on divergent laser beam to the measurement of the angle of arrival fluctuations and the refractive index structure constant in the turbulent atmosphere," Opt. Lett. **33**, 980–982 (2008).
17. F. L. Pedrotti and L. S. Pedrotti, *Introduction to Optics* (Prentice Hall, 1993).
18. T. Du and W. Luo, "Nonlinear optical effects in ferrofluids induced by temperature and concentration cross coupling," Appl. Phys. Lett. **72**, 272–274 (1998).